CSTAM 2012-D01-0018

Contact Mechanics in Flexural MEMS Stiction

Yin Zhang, Ya-Pu Zhao

State Key Laboratory of Nonlinear Mechanics,
Institute of Mechanics
Chinese Academy of Sciences

第十二届全国物理力学学术会议
2012 年 11 月 12—13 日 广西·桂林

CSTAM2012-D01-0018

Contact Mechanics in Flexural MEMS Stiction[1)]

Yin Zhang[*, 2)], Ya-pu Zhao[*]

*(State Key Laboratory of Nonlinear Mechanics (LNM), Institute of Mechanics, CAS, Beijing 100190)

Abstract A variational method using the principle of virtual work (PVW) is presented to formulate the problem of the microcantilever stiction. Compared with the Rayleigh–Ritz method using the arc-shaped or S-shaped deflection, which prescribes the boundary conditions and thus the deflection shape of a stuck cantilever beam, the new method uses the matching conditions and constraint condition derived from PVW and minimization of the system free energy to describe the boundary conditions at the contact separation point. The transition of the beam deflection from an arc-shape-like one to an S-shape-like one with the increase of the beam length is shown by the new model. The (real) beam deflection given by this new model deviates more or less from either an arc-shape or an S-shape, which has significant impact on the interpretation of experimental data. The arc-shaped or S-shaped deflection assumption ignores the beam bending energy inside the contact area and the elastic energy due to the beam/substrate contact, which is inappropriate as shown by this study. Furthermore, the arc-shaped or S-shaped deflection only approximately describes the deflection shape of a stuck beam with zero external load and obviously, the external load changes the beam deflection. The Rayleigh–Ritz method using the arc-shaped or S-shaped deflection assumption in essence can only be used to tell approximately whether stiction occurs or not. Rather than assuming a certain deflection shape and by incorporating the external load, the new method offers a more general and accurate study not only on the microcantilever beam stiction but also on its de-adherence.

Keywords Stiction, Adhesion, Microcantilever, Interface

Introduction

Stiction is one of the most widespread hazards threatening the reliable operation of the micro-electromechanical systems (MEMS) devices [1, 2]. Stiction is often categorized as release-related stiction and in-use stiction [1, 3]. The capillary force [1,2,4,6–9], electrostatic force [4,9–13], mechanical load [14] and inertial forces [8] during the MEMS release or in-use stage can all be the actuation mechanisms to bring the devices into contact with one another or with the substrate. The system free energy of the device in contact consists of two parts: the mechanical energy and surface energy. Adhesion energy is defined as the reduction of the surface energy per unit area when combining two surfaces into one interface [15], which is also referred to as the surface interaction energy [1,2]. Once the external load is retracted, two things happen in terms of the system free energy: the increase of the mechanical energy due to the device deformation and the decrease of the surface energy due to adhesion. In terms of force, the device deformation generates a restoring force to try to pull the device back to the free-standing state; the tensile pressure around the contact separation edge [16, 17] due to adhesion tries to balance the restoring force and keeps the devices in a deformed state. The competition between the mechanical and surface energies determines whether stiction occurs or not. Here the stiction state is defined as an attachment state after the external/actuation load is retracted. Therefore, the external load does not appear as a parameter in many stiction studies [7, 8, 18]. The stable equilibrium of a stiction state corresponds to a local minimum of the system total free energy [5,18] and there is no stiction if such local minimum does not exist [18]. The peel number of N_P [18], which is defined as a convenient way to tell whether

1) This project was supported by the National Natural Science Foundation of China (10721202 and 10772180)
2) Email: zhangyin@lnm.imech.ac.cn

stiction occurs or not, is given as follows for a cantilever beam

$$N_{\mathrm{P}} = C\frac{E_1 T^3 H^2}{\gamma_{\mathrm{s}} L_{\mathrm{u}}^4} \quad (1)$$

C is a constant. E_1, T and L_u are Young's modulus, thickness and unstuck length of the cantilever, respectively. H is the gap distance between the undeformed beam and substrate as shown in Fig. 1(a). γ_s is the adhesion energy. Stiction occurs when $N_P \leq 1$ and no stiction when $N_P > 1$ [18]. $N_P = 1$ corresponds to the cantilever equilibrium obtained by minimizing the system free energy as shown in Appendix A. The dimensionless peel number can also be viewed as the order of the ratio of the mechanical energy to the surface energy [2, 19].

However, the inconsistency and unreliability of the experimental data obtained in the beam stiction test using above Eq. (1) have been noticed [1, 23]. Van Spengen et al. [1] concluded that "the surface interaction energy measurement using stuck beams needs considerably more research before we can conclude anything definite about the precise magnitude of the measured surface interaction energy". Most of the previous studies, according to van Spengen et al. [2], have "never come further than a peel number". A more comprehensive way of studying the beam stiction should include the effect of surface roughness [1, 2, 23], whose distribution determines how two surfaces contact each other. A more accurate description on the stuck beam deflection in essence only offers a better characterization of the nominal adhesion energy. However, it is still a valuable tool and allows us to observe trends [1]. The principle of virtual work (PVW) is used in this study to derive the governing equation and matching/boundary conditions of a stuck cantilever. Unlike that an arc-shape or an S-shape specifies the boundary conditions at the contact separation points, the matching conditions determine what kind of the boundary conditions should be formed at the contact separation point, which are neither hinged nor clamped. The model presented here incorporates the cantilever beam dimensions, adhesion and external load and shows how these quantities change the beam deflection shape rather than prescribing it. By doing so, a more general and accurate method of describing the stuck cantilever deflection is presented.

1. Model Development

The bending energy U_B, which consist of both unstuck and stuck parts, is the following

$$U_{\mathrm{B}} = \frac{E_1 I}{2}\int_0^L \frac{\mathrm{d}^2 W}{\mathrm{d}x^2}\mathrm{d}x = \frac{E_1 I}{2}\left(\int_0^{x_1}\frac{\mathrm{d}^2 W_1}{\mathrm{d}x^2}\mathrm{d}x + \int_{x_1}^L \frac{\mathrm{d}^2 W_2}{\mathrm{d}x^2}\mathrm{d}x\right) \quad (2)$$

U_F of the energy stored by the elastic foundation due to the beam/substrate contact is given as follows:

$$U_{\mathrm{F}} = \frac{k}{2}\int_{x_1}^L (W_2 - H)^2\,\mathrm{d}x \quad (3)$$

H is the gap distance between the undeformed beam and substrate as shown in Fig. 1(a) and k is the modulus of elastic foundation. Eq. (3) indicates that the potential energy is stored by a series of springs with stiffness k.

The surface energy, U_S, is given as the following [5,7,18]

$$\mathrm{U_S} = -2\mathrm{B}\gamma_{\mathrm{s}}(\mathrm{L} - \mathrm{x_1}) \quad (4)$$

2B is the beam width and $L - x_1$ is the beam contact length. $2B(L - x_1)$ is thus the contact/stuck area. γ_s is the adhesion energy between the beam and substrate, which is also known as the surface interaction energy [1,2] and the Dupré work of adhesion [19]. It is noticed that U_S is negative, which physically means that the system free energy reduces when combining two sur-faces into one interface [15].

This reduction of surface energy is the mechanism responsible for the microstructure stiction. On the other side, the restoring force due to the mechanical energy (U_B and U_F) tries to pull the beam back to the free-standing state. U_{Force}, the work done by P and q, is given as follows:

$$\mathrm{U_{Force}} = \int_0^{\mathrm{W}} \mathrm{q}\,\mathrm{dW} + \int_0^{\mathrm{W}} \mathrm{P}\delta_{\mathrm{D}}(\mathrm{x} - \mathrm{x_0})\mathrm{dW} \quad (5)$$

Here the nondimensionalization scheme is given as follows:

$$\xi = \beta \mathrm{x}, \mathrm{w_i} = \beta \mathrm{W_i}\ (\mathrm{i} = 1,2), \xi_1 = \beta \mathrm{x_1}, \mathrm{h} = \beta \mathrm{H}, \mathrm{l} = \beta \mathrm{L}, \mathrm{F} = \frac{\mathrm{P}}{4\beta^2 \mathrm{E_1 I}}, \mathrm{Q} = \frac{\mathrm{q}}{\beta^3 \mathrm{E_1 I}} \quad (6)$$

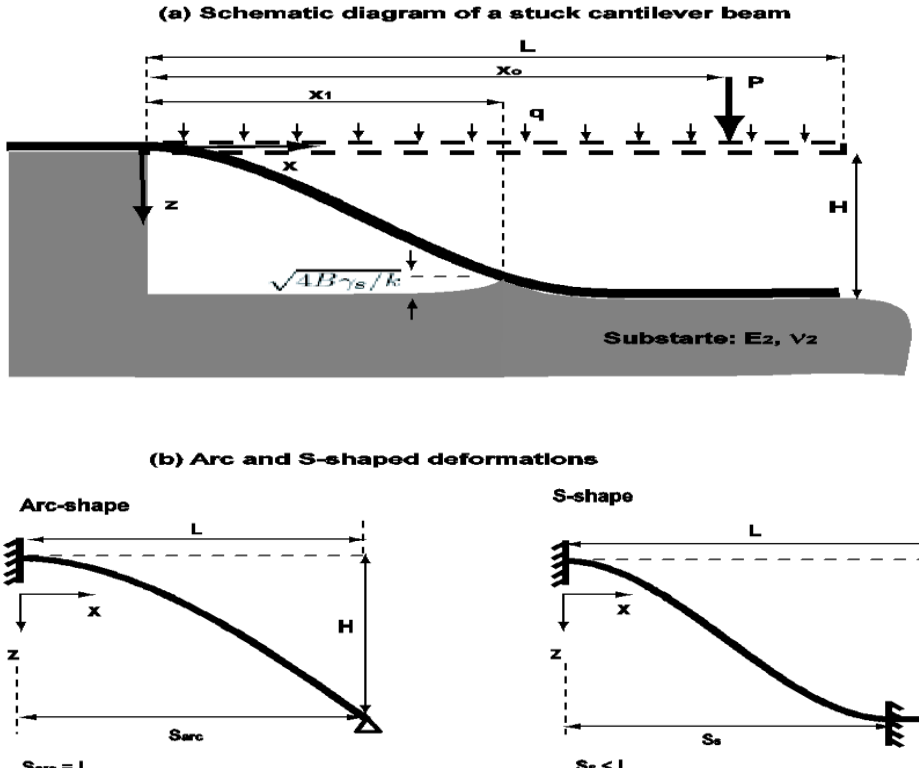

Fig. 1. (a) The schematic diagram of a stuck cantilever under a concentrated load P and a uniformly distributed load q. L is the beam length and H is the gap distance; x_0 is the location of P and x_1 is the separation point. (b) The arc-shaped and S-shaped deflections. S_{arc} and S_{S} are the unstuck lengths of an arc-shape and an S-shape.

Here β is defined as $\beta = 4\sqrt{\frac{\mathrm{k}}{4\mathrm{E_1I}}}$. By using the nondimensionalization scheme of Eq. (6) and applying the principle of virtual work (PVW) [25, 26], i.e., $(U_{\mathrm{B}} + U_{\mathrm{F}} + U_{\mathrm{S}} - U_{\mathrm{Force}}) = 0$, the following dimensionless governing equations and matching/boundary conditions are obtained

$$\begin{cases} \frac{\mathrm{d}^4 w_1}{\mathrm{d}\xi^4} = Q, & 0 < \xi < \xi_1, \\ \frac{1}{4}\frac{\mathrm{d}^4 w_1}{\mathrm{d}\xi^4} + w_2 - h = \frac{Q}{4} + F\delta_D(\xi - \xi_0), & \xi_1 \le \xi \le l, \end{cases} \tag{7}$$

$$w_1(\xi_1) = w_2(\xi_1),\ \frac{\mathrm{d}w_1}{\mathrm{d}\xi}(\xi_1) = \frac{\mathrm{d}w_2}{\mathrm{d}\xi}(\xi_1),\ \frac{\mathrm{d}^2 w_1}{\mathrm{d}\xi^2}(\xi_1) = \frac{\mathrm{d}^2 w_2}{\mathrm{d}\xi^2}(\xi_1),\ \frac{\mathrm{d}^3 w_1}{\mathrm{d}\xi^3}(\xi_1) = \frac{\mathrm{d}^3 w_2}{\mathrm{d}\xi^3}(\xi_1)\,, \tag{8}$$

$$w_1(0) = 0,\ \frac{\mathrm{d}w_1}{\mathrm{d}\xi}(0) = 0,\ \frac{\mathrm{d}^2 w_1}{\mathrm{d}\xi^2}(l) = 0,\ \frac{\mathrm{d}^3 w_1}{\mathrm{d}\xi^3}(l) = 0\,, \tag{9}$$

At the separation point, a constraint condition can be derived as follows via a fracture mechanics approach

$$w_2(\xi_1) = h - \frac{\sqrt{\alpha}}{2} \tag{10}$$

Here α is defined as $\alpha = \frac{4\beta\gamma_{\mathrm{S}}}{E_1 I \beta^2}$. Eq. (7) is the governing equation, which consists of two fourth order differential equations. Therefore, there are eight unknowns due to the two fourth order differential equations plus that the separation point, ξ_1, is also unknown; there are nine unknowns in total. Eqs (8), (9) and (10) offer nine equations in total and the problem can thus be solved via Neewton-Rhapson method. The detailed procedures can be found in references [?].

2. Results and Discussion

Figure 2 compares the stiction shape derived by this new method with the arc- and S-shaped deflections, which are described by Eqs. (47) and (48) in Appendix A, respect-tively.

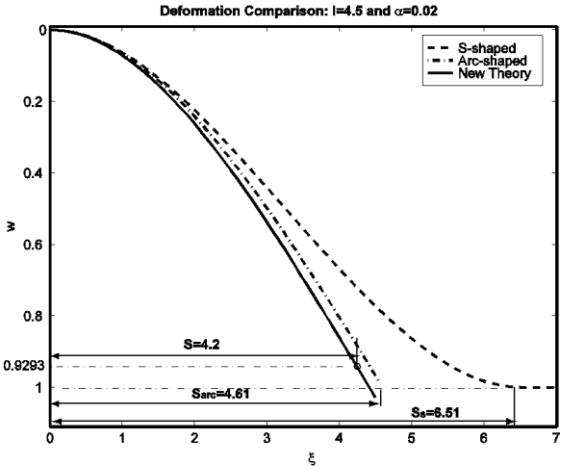

Fig. 2. Deflection comparison of a "chunky" beam ($l = 4.5$ and $\alpha = 0.02$), arc-shape and S-shape.

Clearly, our stiction shape is different from either arc-shape or S-shape. It is noticed that the beam predicted by our model separates from the substrate with the vertical displacement of $h - \frac{\sqrt{\alpha}}{2} \approx 0.929\,3$; the vertical displacements at the separation points are h = 1 for both arc- and S-shapes. The contact zone is now divided into two parts in terms of contact pressure: a zone around the beam free end (i.e., $w(\xi) > 1$) is with compressive pressure and a zone around the contact separation point (i.e., the zone of $0.929\,3 \leq w(\xi) < 1$) is with tensile pressure. This resembles the Johnson – Kendall – Roberts (JKR) contact scenario of two spheres: The inner circular zone is with compressive pressure and outer annulus zone is with tensile pressure [16,17]. In terms of force equilibrium, the tensile pressure due to adhesion in the zone around the contact separation point balances the restoring forces due to the beam bending and contact deformations. The beam length of $l = 4.5$ is smaller than S_{arc} and S_{s}. Therefore, if either an arc-shape or an S-shape assumption is used to predict the beam stiction, the beam with $l = 4.5$ and $\alpha = 0.02$ can not adhere to the substrate. In our computation, this $l = 4.5$ is the critical length and no stiction can occur with the length shorter than this value. Clearly, in Fig. 3 the arc-shape deflection is a much better approximation than S-shape for the (real) beam stiction shape.

Figure 3 compares the stiction shape ($F = Q = 0$) of a slender beam with arc- and S-shapes. With the fixed values of $h = 1$ and $\alpha = 0.02$, the unstuck lengths, $S_{\text{arc}} = 4.61$ and $S_{\text{s}} = 6.51$ of arc-shape and S-shapes, respectively, remain unchanged. Now the S-shape closely matches the deflection curve of the new model. There is only some small difference in the contact area. Again, with the fixed values of h and α the deflection curve of the new model separates from the substrate with the same vertical displacement of 0.929 3. But the unstuck length changes as $\xi_1 = 5.49$. The advantage of the new model is now standing out: rather than prescribing the boundary conditions at the separation point as done by the arc-shape and S-shape, the new model configures its deflection through the matching conditions and constraint conditions. It is also worth emphasizing that though the stiction shape of the new model closely matches the S-shape, their unstuck lengths are different, which has significant impact on the interpretation on the adhesion energy measurement.

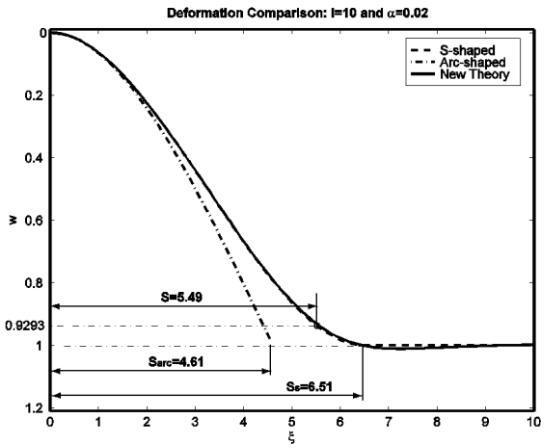

Fig. 3. Deflection comparison of a slender beam ($l = 10$ and $\alpha = 0.02$), arc-shape and S-shape.

3. Summary

A general approach of studying the micro-cantilever stiction is presented. The principle of virtual work is used to derive the governing equation by assuming the deflection shape with a noncontact – contact configuration. The minimization of the system free energy results in the constraint condition, which determines the separation point. This new approach shows that the deflection shape of a stuck cantilever beam is a function of the beam dimensions and mechanical properties, gap distance, adhesion, loading type and magnitude. The transition and change of the cantilever deflection shape are demonstrated by changing the beam dimensions and loadings. In comparison, the arc-shaped and S-shaped deflections only offer an approximation for the zero loading case, which deviates more or less from the one predicted by this approach.

The difference of the deflection shapes has a direct impact on the calculation of the system energy and thus the interpretation of experimental data. In essence, this new approach offers a more accurate model on the stuck cantilever by not prescribing its deflection shape.

Acknowledgments

This project was supported by the National Natural Science Foundation of China (10721202 and 10772180).

References

[1] W.M. van Spengen, R. Puers, I. De Wolf, A physical model to predict stiction in MEMS, J. Micromech. Microeng. 12 (2002) 702–713.

[2] W.M. van Spengen, R. Puers, I. De Wolf, The prediction of stiction failures in MEMS, IEEE Trans. Dev. Mater. Reliab. 3 (2003) 167–172.

[3] R. Maboudian, R.T. Howe, Critical review: adhesion in surface micromechanical structures, J. Vac. Sci. Technol. B 15 (1997) 1–20.

[4] N. Tas, T. Sonnernberg, H. Jansen, R. Legtenberg, M. Elwenspoek, Stiction in surface micromaching, J. Micromech. Microeng. 6 (1996) 385–397.

[5] F. Yang, Contact deformation of a micromechanical structure, J. Micromech. Microeng. 14 (2002) 263–268.

[6] C.H. Mastrangelo, C.H. Hsu, Mechanical stability and adhesion of microstructures under capillary forces – part I: basic theory, J. Microelectromech. Syst. 2 (1993) 33–43.

[7] R. Legtenberg, T. Tilmans, J. Elders, M. Elwenspoek, Stiction of surface micromachined structures after rinsing and drying: model and investigation of adhesion mechanisms, Sens. Actuators A 43 (1994) 230–238.

[8] M.P. de Boer, T.A. Michalske, Accurate method for determining adhesion of cantilever beams, J. Appl. Phys. 86 (1999) 817–827.

[9] M.P. de Boer, J.A. Knapp, T.M. Mayer, T.A. Michalske, The role of interfacial properties on MEMS performance and reliability, Proc. SPIE 3825 (1999) 2–15.

[10] J.A. Knapp, M.P. de Boer, Mechanics of microcantilever beams subjected to combined electrostatic and adhesive forces, J. Microelectromech. Syst. 11 (2002) 754–764.

[11] Y. Zhang, Y.P. Zhao, Static study of cantilever beam stiction and electrostatic force influence, Acta Mech. Solida Sin. 17 (2004) 104–112.

[12] Y. Zhang, Y.P. Zhao, Vibration of an adhered microbeam under a periodically shaking electrical force, J. Adhes. Sci. Technol. 19 (2005) 799–815.

[13] A. Savkar, K.D. Murphy, Z.C. Leseman, T.J. Mackin, M.R. Begley, On the use of structural vibrations to release stiction failed MEMS, J. Microelectromech. Syst. 16 (2007) 163–173.

[14] E.E. Jones, M.R. Begley, K.D. Murphy, Adhesion of micro-cantilever subjected to mechanical point loading: modeling and experiments, J. Mech. Phys. Solids 51 (2003) 1601–1622.

[15] H.H. Yu, Z. Suo, A model of wafer bonding by elastic accommodation, J. Mech. Phys. Solids 46 (1998) 829–844.

[16] K.L. Johnson, Contact Mechanics, Cambridge University Press, Cambridge, 1985 (Chapter 5).

[17] Y. Zhang, Transitions between different contact models, J. Adhes. Sci. Technol. 22 (2008) 699–715.

[18]C.H. Mastrangelo, C.H. Hsu, Mechanical stability and adhesion of microstructures under capillary forces – part II: experiments, J. Microelectromech. Syst. 2 (1993) 44–55.

[19] Y.P. Zhao, L.S. Wang, T.X. Yu, Mechanics of adhesion in MEMS – a review, J. Adhes. Sci. Technol. 17 (2003) 519–546.

[20] Y. Zhang and Y.P. Zhao, A Precise Model for the Shape of an Adhered Microcantilever, Sensors and Actuators A: Physical, 171 (2011) 381-390.

[21] Y. Zhang and Y.P. Zhao, Flexural contact in MEMS stiction, International Journal of Solids and Structures (in press).